

INTERPRETATION OF MERCURY INJECTION EXPERIMENTS USING A MINIMUM SET OF POROUS DESCRIPTORS DERIVED BY QUANTITATIVE IMAGE ANALYSIS

YANNICK ANGUI¹, SOPHIE BELIN¹, ROBERT EHRLICH² AND AZITA AHMADI¹

¹LEPT-ENSAM, UMR 8508, Esplanade des Arts et M&iers, 33405 Talence cedex France, ²Residuum Energy, 1048 S Oak Hills Way, Salt-Lake City, USA

e-mail: yannick@lept-ensam.u-bordeaux.fr, bobehlich@attbi.com

(Accepted May 28, 2002)

ABSTRACT

The porosity exposed in a series of petrographic thin sections from a sub-arkosic sandstone reservoir of the Alwyn area (North Sea) is described by 5 morphological porous descriptors, Pore-Types, obtained by quantitative image analysis procedures and pattern recognition algorithms developed by Ehrlich *et al.* (1991a). By combining Pore-Type data with capillary pressure curves, we obtain preliminary results showing that in the studied reservoir, the achieved Pore-Types relate better to petrophysics when they are complemented with a sedimentological information.

Keywords: capillary pressure curves, connectivity, morphology, Pore-Types, sandstone, throats.

INTRODUCTION

For a variety of transport processes in porous media, there exists a strong relation between the structure at the pore-scale and the macroscopic transport properties. The comprehensive and predictive study of such relation requires the availability of analytical models relating the physical property of interest to a minimum set of geometrical parameters describing those aspects of the fabric relevant to physics.

As far as sedimentary detritic granular rocks such as sandstones are concerned, a variety of studies converged towards a general structural model where the pore space is partitioned into a few classes of porosity whose size and shape are controlled by the dynamics of the aggregation (Graton and Fraser, 1935; Berg, 1975; Ehrlich *et al.*, 1991a,b; McCreech *et al.*, 1991; Prince *et al.*, 1995). This general model, illustrated qualitatively in Fig. 1 by an experiment with a mono layer of spheres, highlights two classes of porosity: 1 loose-packed pores, and 2 close-packed pores.

Graton and Fraser (1935) acknowledged first the inevitable occurrence of this domainal structure arising from the dynamics of the sedimentation: due to the simultaneous sedimentation of the grains, many foci of close packing form simultaneously, but no process exists to insure the mutual, parallel alignment of their internal fabrics. As the well-packed clusters grow towards another, an intervening compromise

zone of loose-packing is formed. This fabric was generalized into 3-D by Azaroff (1960).

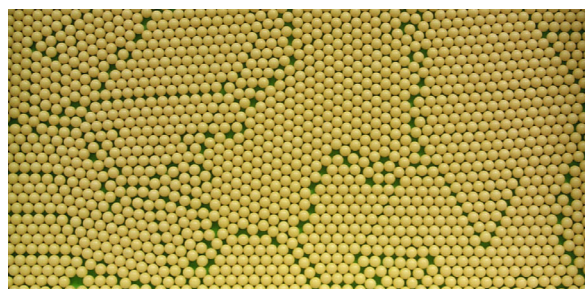


Fig. 1. General model for the structure of sedimentary granular rocks.

In the structural model above, packing (and grain size) control both pore size and throat allowing pores of like type to be mutually adjacent (in the form of continuous circuits or within well-packed clusters of grains) and connected by similarly sized throats (Graton and Fraser, 1935; Berg, 1975; McCreech *et al.*, 1991). Thus, at the time of deposition, pores of like type determine the flow paths. Of course, the influence of pores of like type on the flow-paths may then be weakened by the diagenetic overprint. Yet, the availability of this general structural model suggests that a set of porous descriptors will show a petrophysical relevance if they describe the different classes of porosity illustrated in Fig. 1.

Ehrlich *et al.* (1991a) devised an automatic procedure where the porosity of a sample suite is

classified into a few classes of objects, called Pore Types. Pore Types are derived from the size and shape (the morphology) of the PORE ELEMENTS (porels) exposed in a series of petrographic thin sections and are interpreted as the consequence of the depositional and post-depositional processes at the origin of the rock. The petrophysical relevance of Pore Types has been quantified for a variety of sandstone reservoirs in the form of the association between Pore Types and throat size, obtained by blending Pore Type data with capillary pressure data (McCreesh *et al.*, 1991). The "Pore Types / throat size" relation yielding all the necessary information to parameterize physical models of tube-like type, the effects of Pore Types on physical properties such as permeability, formation factor etc. ... have been documented for a variety of case studies (Ehrlich *et al.*, 1991b).

This work is an application of the Ehrlich *et al.* (1991a, b) and McCreesh *et al.* (1991) approach to a series of sub-arkosic sandstone samples from the Brent of the Alwyn area (North Sea) showing various amounts of kaolinite and illite (Belin *et al.*, 1999). In a previous contribution (Anguy *et al.*, 1999), we showed that, for this particular reservoir, the achieved Pore Types were not sufficient to interpret a series of capillary pressure curves measured on the plugs from which were cut the thin sections used to determine the Pore Types. The objective of the current work is to evaluate if such an interpretation becomes possible when the sedimentological context associated to the Pore Types is taken into account. The sedimentological information considered herein being incomplete, this work is a preliminary report.

GEOMETRICAL CHARACTERIZATION

Ehrlich *et al.* approach (1991a) relies on the idea that the multitude of elementary closed loops of porosity (PORE ELEMENTS: porels) observed in a thin section such as Fig. 2 is the 2-D signature of a few classes of 3-D objects, or Pore Types, intersected by the plane of section.

Pore Types determination requires the availability of a series of \mathcal{M} thin sections. For each thin section, a statistically significant number of porels are submitted to erosion / dilation (ED) procedures where each porel is smoothed by progressive degrees of erosion followed by an equal degree of dilation. The number of pixels lost between successive ED cycles is recorded as a frequency roughness. The ED process stops as the number of erosions exceeds half the maximum width of the porel, the final dilation supplying the smooth part of the porel. The frequency

distribution of size and shape of the thin section is produced by pooling all porel smooth/rough spectra and converting pixel frequencies to proportions.

The \mathcal{M} frequency distribution of size and shape are the input data to a pattern recognition / classification algorithm whose output expresses the porosity of the sample set as a linear mixture of N Pore Types (Eq. 1) (Miesch, 1976; Klovan and Miesch, 1976; Full *et al.*, 1981).

$$Q = A.F, \quad (1)$$

where: Q is a $\mathcal{M} \times \mathcal{V}$ matrix whose i^{th} row is a i^{th} frequency distribution of size and shape with \mathcal{V} class intervals, each interval relating to a range of sizes of roughness (resp. smooth seed). A is a $\mathcal{M} \times N$ matrix whose element a_{ik} is the proportion of the k^{th} Pore Type in the i^{th} sample. F is a $N \times \mathcal{V}$ matrix whose element f_{kj} is the proportion of j^{th} class interval in the k^{th} Pore Type.

Five Pore Types $PT_{i=1,5}^i$ (Figs. 3-7) were obtained to describe the porosity of the 27 available thin sections (Anguy *et al.*, 1999). The porels characteristic of a PT can be visualized on the digital binary images containing the PT in a high proportion and the PT can be replaced in its sedimentological framework(s) by examining the corresponding petrographic thin section.

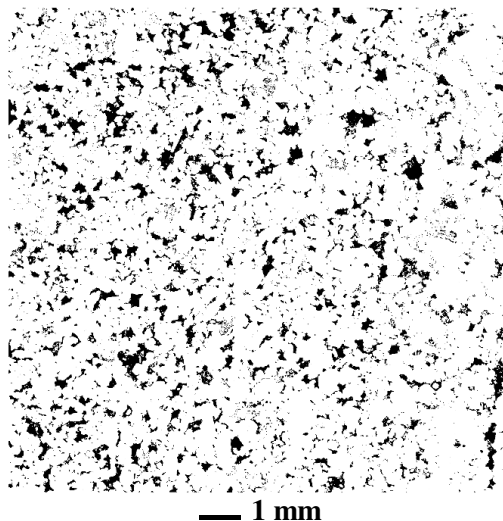


Fig. 2. 1981×2047 binary image of a sandstone from the Tarbert Formation. Image Size: 10.3×10.7 mm; pixel size: $5.208 \mu\text{m}$. Optical porosity (≈ 0.125) expressed by black. The image is acquired on a Scanning Electron Microscope (SEM) in back-scattered mode and consists of 5×5 elementary overlapping views, each 512×512 pixels, binarized, and then merged into a mosaic.

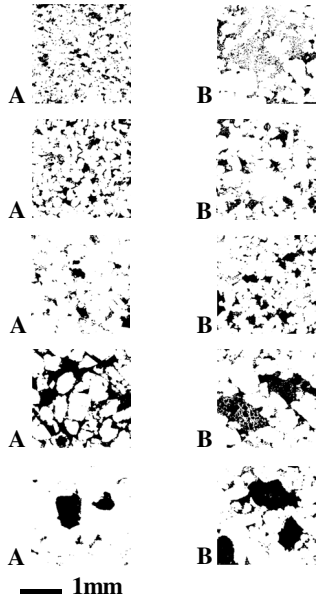


Fig. 3. Pore Type 1. A: Intergranular primary pores at grain boundaries within well-packed local clusters of grains. B: Small intra-particle pores in partially dissolved feldspars containing flaky clusters of illite.

Fig. 4. Pore Type 2. A-B: Primary intergranular porosity ("packing flaws") located essentially in contact zones between clusters of efficiently packed grains.

Fig. 5. Pore Type 3. A: Primary intergranular porosity. B: Dissolved feldspars.

Fig. 6. Pore Type 4. A: Very connected primary intergranular porosity ("packing flaws"). B: Dissolved feldspars filled by flaky clusters of illite.

Fig. 7. Pore Type 5. A-B: Very large pores associated to dissolved feldspars.

The optical porosity of the sample in Fig. 2 contains the 5 PTs in the following proportions: PT¹: 0.19, PT²: 0.09, PT³: 0.43, PT⁴: 0.24 and PT⁵: 0.05.

DISCUSSION

PETROPHYSICAL RELEVANCE OF THE POROUS DESCRIPTORS

The petrophysical relevance of PTs has been quantified for various reservoirs by relating PT data (matrix \underline{A} in Eq. 1) to mercury capillary pressure (P_c) data measured on the plugs from which the available thin sections were cut (McCreesh *et al.*, 1991).

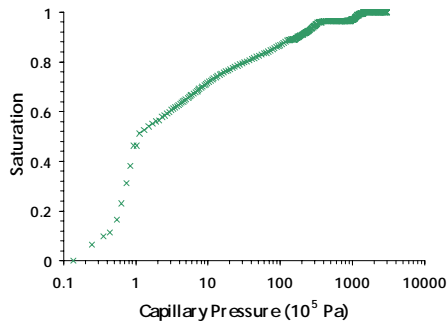


Fig. 8. Capillary pressure (P_c) curve measured on the plug from which was cut the thin section displayed in Fig. 1. Crosses represent experimental mercury saturations as a function of capillary pressure.

A P_c curve (Fig. 8) is a macroscopic measure of the fraction of porosity (saturation) invaded by mercury as a function of pressure. For constant surface tension (480 mN.m⁻¹) and contact angle for mercury ($\theta = 141.3$ degrees), P_c relates to throat size according to $P_c = 7.492 \cdot 10^5 \cdot r^{-1}$ (P_c in Pa and r in μm). Fig. 8 is

accordingly a measure of the fraction of porosity lying behind throats of a given size.

The relation between PTs and throat size is searched in the form of a series of equations representing the relative filling of the Pore Types as a function of P_c (Eq. 2):

$$\begin{pmatrix} S_i^1 \\ S_i^2 \\ \vdots \\ S_i^j \\ \vdots \\ S_i^M \end{pmatrix} = \begin{pmatrix} a_{11} & a_{12} & \cdots & a_{1k} & \cdots & a_{1N} \\ a_{21} & a_{22} & \cdots & a_{2k} & \cdots & a_{2N} \\ \vdots & \vdots & & \vdots & & \vdots \\ a_{j1} & a_{j2} & \cdots & a_{jk} & \cdots & a_{jN} \\ \vdots & \vdots & & \vdots & & \vdots \\ a_{M1} & a_{M2} & \cdots & a_{Mk} & \cdots & a_{MN} \end{pmatrix} \begin{pmatrix} \alpha_i^1 \\ \alpha_i^2 \\ \vdots \\ \alpha_i^k \\ \vdots \\ \alpha_i^N \end{pmatrix}, \quad (2)$$

where: S_i^j is the relative saturation recorded for a j^{th} sample in a i^{th} discrete pressure interval representing a range of throat sizes. Coefficient a_{jk} is the proportion of the k^{th} PT in the j^{th} sample (Eq. 1)

In Eq. 2, α_i^k is the searched fraction of a k^{th} Pore-Type invaded by mercury in a i^{th} P_c interval. For a series of discrete P_c intervals, the unknowns of the model (α_i^k) are determined by a maximum likelihood estimator strategy. The correctness of the obtained relation between PTs and throat size (the achieved model of connectivity) can be checked by calculating simulated P_c curves from the determined α_i^k ($k=1, N; i=1, M$ and \underline{A} matrix (N: number of PTs; M number of discrete P_c intervals).

The studied samples show a variable amount of illite or kaolinite. For each sample, the associated micro-porosity, not resolved in a binary image such as Fig. 2, was estimated in the manner of Sears (1984) from measured thin section clay content. A *pseudo* Pore Type PT^0 was introduced in the right hand side of Eq. 2 allowing: 1. to take into account the estimated micro-porosity fraction, and 2. to re-scale, to a first approximation, fractions of optical porosity (matrix A) to fractions of porosity seen by mercury (vector S_i in Eq. 2).

In a previous study (Anguy *et al.*, 1999), we solved Eq. 2 for 15 discrete P_c bins in order to interpret the measured P_c curves in terms of the relative filling of the 5 PTs. The achieved model of accessibility, provided in Fig. 9A, did not permit to reproduce several experimental P_c curves as illustrated in Figs. 10-13 and 15.

Implicit to searching the PTs / throat size relation is that such relation is fixed in all samples of the series (McCreesh *et al.*, 1991). We saw previously that a single PT can relate to different sedimentological framework (Figs. 3, 5, 6). In this respect, if the sedimentological framework associated to a PT is a factor controlling the fixed nature of the PTs / throat size relation, then the model in Fig. 9A is compromised. This may explain its inability to reproduce some of the experimental P_c curves. As far as PT^4 (Fig. 6) is concerned, the information about its sedimentological interpretations can be fitted straightforwardly in Eq. 2. Indeed, the two sedimentological contexts associated to PT^4 i.e., A: primary intergranular porosity and B: dissolved feldspars, are exclusive in the samples. So that one needs only duplicate PT^4 in two Pore-Types PT^{4A} and PT^{4B} and then set to 0 in every sample the content of the duplicated PT whose sedimentological meaning does not apply to the sample. The following PT contents apply for example to Fig. 2 where PT^4 (24%) is associated to dissolved feldspars: PT^{4A} : 0. and PT^{4B} : 0.24.

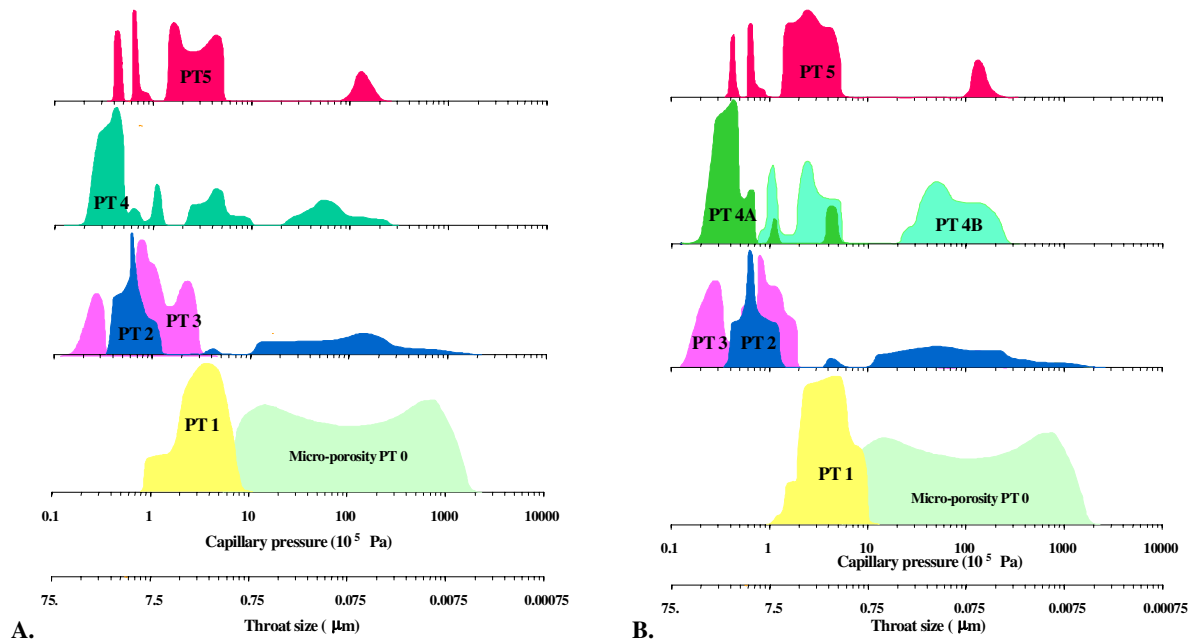


Fig. 9. Relation between PTs and throat size obtained A: by taking into account MORPHOLOGICAL criteria, and B. by taking into account both MORPHOLOGICAL and SEDIMENTOLOGICAL criteria. In A and B, the 15 discrete regression equations predicting the filling of PTs at discrete P_c intervals are schematically represented as continuous distributions of PT volume invaded by mercury as a function of P_c (throat size). For example, in Fig. 9A, PT^4 fills in 3 modes: 60% of PT^4 fill in a $0.32 \cdot 10^5 - 0.64 \cdot 10^5$ P_c range (throat sizes: $23.4 - 11.7 \mu m$), another 16% of PT^4 are invaded by mercury at a P_c range of $1.72 \cdot 10^5 - 8.23 \cdot 10^5$ Pa (throat sizes: $4.4 - 0.9 \mu m$) and another 20% in a P_c range of $14.1 \cdot 10^5 - 749.2 \cdot 10^5$ Pa (throat sizes: $0.5 - 0.01 \mu m$) (Anguy *et al.*, 1999).

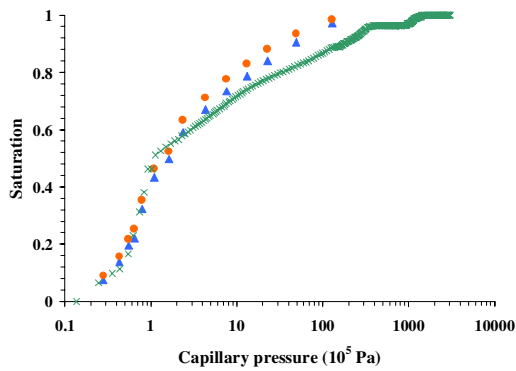


Fig. 10. Sandstone from the Tarbert Formation (Fig. 2) (core depth: 4125 m). Green crosses: experimental mercury saturation as a function of P_c . Orange circles: discrete simulated P_c curve calculated using the model of connectivity in Fig. 9A (Anguy et al. 1999). Blue triangles: discrete simulated P_c curve calculated using the model of connectivity in Fig. 9B.

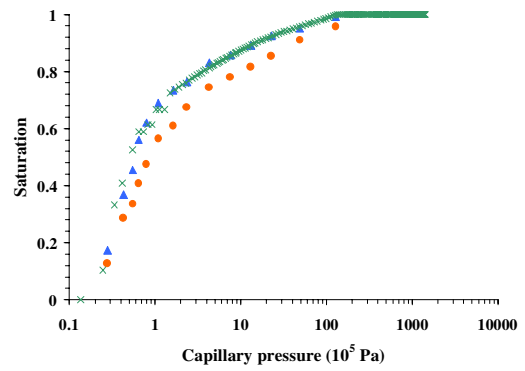


Fig. 13. Same as Fig. 10 but for a sample of the suite from the Ness 1 Unit Formation (core depth: 3585.00 m).

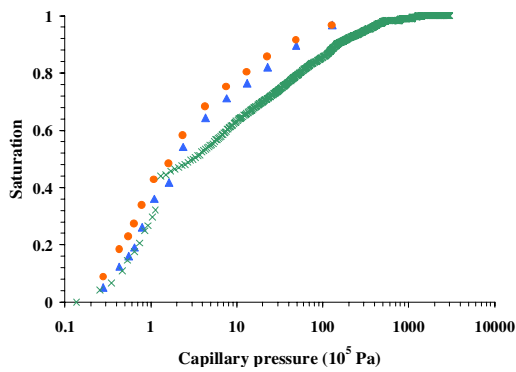


Fig. 11. Same as Fig. 10 but for another sample of the series from the Tarbert Formation (core depth: 3553.30 m).

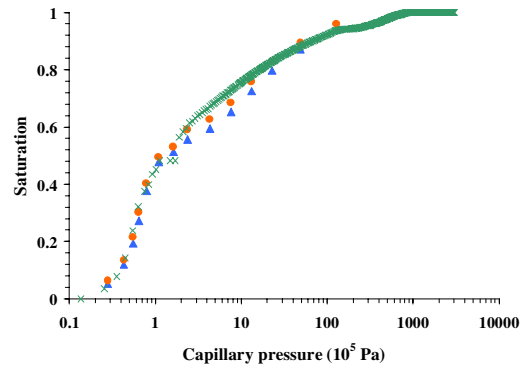


Fig. 14. Same as Fig. 10 but for another sample of the suite from the Ness 2 Unit Formation (core depth: 3195.70 m).

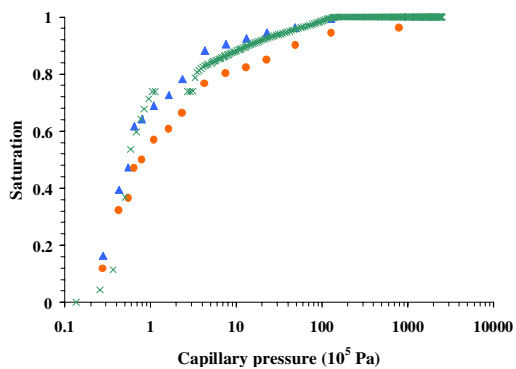


Fig. 12. Same as Fig. 10 for a sample of the suite from the Ness 2 Unit Formation (core depth: 3554.80 m).

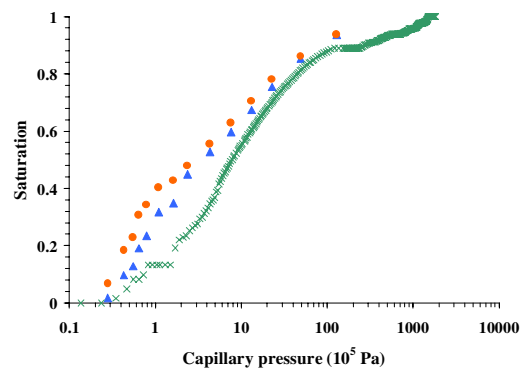


Fig. 15. Same as Fig. 10 but for another sample of the suite from the Tarbert Formation (core depth: 4145.20 m).

We solved again Eq. 2 with PT^4 duplicated according to its two sedimentological meanings and obtain the model of connectivity displayed in Fig. 9B. Experimental P_c curves that were not reproduced by the model in Fig. 9A are now correctly matched (Figs. 12-13). For other samples (Figs. 10, 11 and 15) the differences between measured P_c curves and the simulated P_c curves have been decreased.

This preliminary work suggests that in the case of the studied reservoir, a series of 5 porous descriptors, Pore Types, relate better to petrophysics when the morphological information is complemented by a sedimentological interpretation.

Because the Pore Types / throat size relationship provides all the parameters required by "tube-like" models for permeability, formation factor etc. (Ehrlich *et al.*, 1991b), this suggests that in this reservoir these physical properties arise from both the morphology and the sedimentological context associated to the samples.

REFERENCES

- Anguy Y, Belin S, Bernard D, Fritz B, Ferm JB (1999). Modeling physical properties of sandstone reservoirs by blending 2D image analysis data with 3D capillary pressure data. *Phys Chem Earth (A)* 24(7):581-6.
- Azaroff LB (1960). *Introduction to solids*. McGraw-Hill, New York.
- Belin S, Anguy Y, Bernard D, Fritz B, Ferm JB (1999). Caractérisation par analyse d'images de la micro-géométrie d'un réservoir gréseux illitifié (Alwyn, Mer du Nord). *Bull Soc Geol France* 170(3):367-77.
- Berg RR (1975). Capillary pressures in stratigraphic traps. *Am Assoc Petr Geol Bull* 59(6):939-56.
- Ehrlich R, Crabtree SJ, Horkowitz KO, Horkowitz JP (1991a). Petrography and reservoir physics I: objective classification of reservoir porosity. *Am Assoc Petroleum Geol Bull* 75(10):1547-62.
- Ehrlich R, Etris EL, Brumfield D, Yan LP, Crabtree SJ (1991b). Petrography and reservoir physics III: physical models for permeability and formation factor. *Am Ass Petr Geol Bull* 75(10):1579-92.
- Full WE, Ehrlich R, Klovan JE (1981). Extended Qmodel - objective definition of external end members in the analysis of mixtures. *J Math Geol* 13(4):331-44.
- Graton LC, Fraser HJ (1935). Systematic packing of spheres with particular relation to porosity and permeability. *J Geology* 43:785-909.
- Klovan JE, Miesch AT (1976). Extended CABFAC and QMODEL computer programs for Q-mode factor analysis of compositional data. *Comput Geosci* 1:61-76.
- McCreech CA, Ehrlich R, Crabtree S (1991). Petrography and reservoir physics II: relating thin section porosity to capillary pressure, the association between pore types and throat sizes. *Am Assoc Petr Geol Bull* 75(10):1563-78.
- Miesch AT (1976). Q-mode factor analysis of geochemical and petrologic data matrices with constant row sums. *US Geol Survey Prof Paper*, 574G, 47pp.
- Prince CM, Ehrlich R, Anguy Y (1995). Analysis of spatial order in sandstones II: grain clusters, packing flaws, and the meso-scale structure of sandstones. *J Sedim Research* A65(1):13-28.
- Sears SO (1984). Porcelaneous cement and microporosity in California turbidites - origin and effect on reservoir properties. *J Sedim Petr* 54:159-69.